RILUZOLE BLOCKS HUMAN MUSCLE ACETYLCHOLINE RECEPTORS

Cristina Deflorio[1], Eleonora Palma[1,2], Luca Conti[1], Cristina Roseti[1,2], Alessia Manteca[1], Elena Giacomelli[3], Cristina Limatola[1,4], Maurizio Inghilleri[3], Francesca Grassi[1]

[1]Dept. of Physiology and Pharmacology, Sapienza University, Rome, Italy

[2]IRCCS San Raffaele Pisana, Rome, Italy

[3]Dept. of Neurology and Psychiatry, Sapienza University, Rome, Italy

[4]Neuromed IRCCS, Venafro (IS), Italy

Running title: Riluzole blocks human muscle AChR

Key words: muscle AChR; amyotrophic lateral sclerosis; riluzole

Total number of words in the paper: 4250

Corresponding author: Francesca Grassi. Dip. Fisiologia e Farmacologia, Università Sapienza, P.le A. Moro 5; I-00185 Roma, Italy. e-mail: francesca.grassi@uniroma1.it

Table of Contents category: Molecular and cellular

ABSTRACT

Riluzole, the only drug available against amyotrophic lateral sclerosis (ALS), has recently been shown to block muscle ACh receptors (AChR), raising concerns about possible negative side-effects on neuromuscolar transmission in treated patients. In this work we studied riluzole impact on the function of muscle AChR *in vitro* and on neuromuscular transmission in ALS patients, using electrophysiological techniques. Human recombinant AChR composed by $\alpha_1\beta_1\delta$ subunits plus γ or ε subunits (γ- or ε-AChR) were expressed in HEK cells or Xenopus oocytes. In both preparations, riluzole at a clinically relevant concentration reversibly reduced the amplitude and accelerated the decay of ACh-evoked current if applied before coapplication with ACh. The action on γ-AChR was more potent and faster than on ε-AChR. In HEK outside-out patches, riluzole-induced block of macroscopic ACh-evoked current gradually developed during the initial milliseconds of ACh presence. Single channel recordings in HEK cells and in human myotubes from ALS patients showed that riluzole prolongs channel closed time, but has no effect on channel conductance and open duration. Finally, compound muscle action potentials (CMAPs) evoked by nerve stimulation in ALS patients remained unaltered after a 1-week suspension of riluzole treatment. These data indicate that riluzole, while apparently safe on synaptic transmission, may affect the function of AChR expressed in denervated muscle fibres of ALS patients, with biological consequences that remain to be investigated.

ABBREVIATIONS

AChR, acetylcholine receptor; ALS, amyotrophic lateral sclerosis; CMAP, compound muscle action potential; EGFP, enhanced green fluorescent protein; I_{ACh}, ACh-evoked whole-cell current; Q_{ACh}, integral of ACh-evoked whole-cell current; PKC, protein kinase C.

INTRODUCTION

Riluzole is the only drug currently registered to treat patients with Amyotrophic Lateral Sclerosis (ALS), a fatal disease due to selective degeneration of upper and/or lower motoneurones. The compound has several adverse side effects, among which asthenia, that further decrease patients' quality of life, so that a full assessment of its effects might help in devising countermeasures. Riluzole affects the function of a variety of ion channels in neurones and possibly in muscle (Bellingham et al., 2011). In particular, when co-administered with ACh, it impairs the function of recombinant mouse acetylcholine receptors (AChR), although only at very high concentrations (Mohammadi et al., 2002), well beyond the range found in patients' serum (0.5 to 5 μM; Bellingham et al., 2011). Conversely, our group recently observed a strong block of AChR function by clinically used concentrations of riluzole in human muscle preparations obtained from ALS or denervated patients, provided that riluzole was applied before the transmitter (Palma et al., 2011). Since AChRs mediate nerve-muscle communication at the neuromuscular junction and are chronically exposed to riluzole in treated patients, it becomes mandatory to understand whether or not riluzole worsens the compromised neuromuscular transmission in ALS patients, possibly elucidating this effect at the molecular level.

ALS patients experience muscle denervation and reinnervation through collateral sprouting of healthy motor neurones (Eisen and Swash, 2001), which, among many other consequences, affects the composition and distribution of muscle AChR. In innervated fibres, receptors formed by the $\alpha_1\beta_1\varepsilon\delta$ subunits (ε-AChR) are densely packed at the endplate and at the myotendineous junction and virtually absent elsewhere (Katz and Miledi, 1964). In denervated muscle cells, AChRs are formed by $\alpha_1\beta_1\gamma\delta$ subunits (γ-AChR), with an almost uniform distribution over the entire sarcolemma (Witzemann et al., 1991). In ALS patients, both ε- and γ-AChR are present, reflecting the presence of denervated muscle fibres.

In this work we prove that *in vitro* riluzole has differential effects on recombinant human γ- or ε-AChR and provide a characterization of its action at the single channel level in transfected cells and in myotubes derived from ALS patients. Moreover, we analyze the effect of riluzole on nerve-muscle transmission in ALS patients before and during a brief suspension of riluzole treatment, reaching the important conclusion

that treatment does not impair compound muscle action potential (CMAP) generation upon repetitive nerve stimulation.

MATERIALS AND METHODS

Patients recruitment and analysis

Thirty-six patients (14 females) with probable or definite ALS according to El Escorial criteria were recruited and analyzed at the ALS centre of Policlinico Umberto I, Università Sapienza of Rome. Their mean age was 64.5 years (range: 47-78 years). CMAPs were recorded from the abductor digiti minimi and deltoid muscles, by ulnar nerve stimulation at the wrist and axillary nerve at Erb's point, respectively. The amplitudes of the initial negative peaks of the CMAPs were measured and the changes in CMAPs amplitude were analyzed. Repetitive nerve stimulation test was performed on the axillary nerve and the ulnar nerve, with the recording electrode over the deltoid muscle and the abductor digiti minimi muscle, respectively. For each train of repetitive stimuli, the amplitudes of the first and fifth CMAPs were compared, and the resulting decrement of the latter expressed as percentage of the first. All patients were examined before and after a 1-week suspension of riluzole treatment; data values were compared using paired Student's *t*-test. Results were considered to be significantly different when $p < 0.05$.

Needle biopsy was performed as previously described (Palma et al., 2011). The study was authorized by the Ethical Committee of Sapienza University and written informed consent to participate in the study was given by all patients.

Cell culture and AChR expression in cells and oocytes

AChR subunit cDNAs in pRBG4 were kindly provided by Dr A.G. Engel (Mayo Clinic, Rochester, USA).

Human embryonic kidney 293 (HEK) cells were grown in Dulbecco's modified Eagle's medium (DMEM) plus 10% foetal bovine serum (both from Invitrogen, Carlsbad, CA) and 1% penicilline / streptomycine. Cells were plated on poly-L-lysine-coated 35 mm Petri dishes and transiently transfected 24 h later using Lipofectamine 2000 (Invitrogen), adding to each dish 1 μg of each subunit cDNA

plus 0.5 μg cDNA encoding enhanced green fluorescent protein (EGFP). HEK cells were mechanically dissociated and replated onto glass coverslips 24 h before measurements. Routinely, cells were used for electrophysiological experiments 48 to 72 h after transfection, as previously reported (Di Angelantonio et al., 2011). Cultures were maintained in a humidified incubator with 5% CO_2, 37 °C.

Human satellite cells were derived from muscle needle biopsies performed on ALS patients, with their written informed consent. Cells were cultured as previously described (Fucile et al., 2006; Palma et al. 2011); differentiation was induced at approximately 50% confluence by switching to a low-serum medium (DMEM plus 2% horse serum and P/S).

Preparation of Xenopus laevis oocytes and nuclear injection procedures were as detailed elsewhere (Miledi et al. 2006). Oocytes were collected under anaesthesia from frogs that were humanely killed after the final collection.

Patch clamp recordings in cultured cells

Currents were recorded at room temperature (23-27^{o} C) via an Axopatch 200B amplifier (Molecular Devices, Union City, CA, USA), using pCLAMP9 (Molecular Devices). In whole-cell and outside-out recordings cells were continuously superfused using a gravity-driven fast exchanger perfusion system (RSC-200, Bio-Logic, France). Whole-cell recordings were performed in standard external solution containing (mM): 140 NaCl, 2.8 KCl, 2 $CaCl_2$, 2 $MgCl_2$, 10 HEPES/NaOH, 10 glucose, pH 7.3. Patch pipettes (2-5 MΩ tip resistance) contained (mM): 140 CsCl, 5 BAPTA, 10 HEPES-KOH, 2 Mg-ATP, 2 $MgCl_2$, pH 7.3. The patch series resistance was compensated by 80-95% and measurements were performed at a holding potential of -60 mV, unless otherwise indicated. Outside-out recordings were performed at -80 mV using standard external medium; patch pipettes (Sylgard-coated for single-channel recordings) contained (mM): 90 CsCl 90, 50 CsF, 5 BAPTA, 10 HEPES-KOH, 2 Mg-ATP, 2 $MgCl_2$, pH 7.3. The rise-time of the ACh-evoked currents, measured as the interval between 10% and 90% of peak amplitude ranged between 0.8 and 3 ms in outside-out recordings.

Cell-attached recordings were performed using standard external solution or a KCl-based solution (mM): 140 KCl, 2.8 NaCl, 2 $CaCl_2$, 2 $MgCl_2$, 10 glucose, 10 HEPES-

KOH, pH 7.3. Sylgard-coated patch pipettes were filled with the extracellular solution used plus ACh (100 nM) alone or additioned with riluzole (0.5 μM), as indicated.

The decay phase of macroscopic ACh-evoked current (I_{ACh}) was fit using pClamp to a single exponential function:

$$I_{ACh}(t) = I_{plateau} + I_0 e^{-t/\tau} \quad \text{(Equation 1)}$$

Single channel recordings obtained under outside-out or cell-attached conditions were filtered at 5 KHz and sampled at 25 KHz. Data were analysed with pClamp 9, using 50% threshold criterion, omitting events shorter than 0.12 ms, as previously described (Di Castro et al., 2007). In cell-attached recordings, slope conductance was calculated by linear fitting of the unitary amplitudes recorded at least at 3 different pipette potentials for each cell. For outside-out recordings, channel conductance was calculated dividing unitary channel amplitude by pipette potential, taking into account a mean reversal potential of 13 ± 3 mV (mean ± SEM, 14 patches).

All salts were purchased from Sigma Italia (Milano, Italy). Two data sets were considered statistically different when $P< 0.05$ by ANOVA or Student's paired *t* test.

Voltage clamp recordings in oocytes

Membrane currents were recorded from voltage clamped oocytes 2-4 days after injection using two microelectrodes filled with 3 M KCl. The oocytes were placed in a recording chamber (volume, 0.1 ml) and perfused continuously, 8–10 ml/min, with oocyte Ringer's solution (Miledi et al., 2006) at room temperature (20–22°C). Unless otherwise specified, oocytes were voltage-clamped at -60 mV.

The half-inhibitory concentration (IC_{50}) of riluzole and the ACh concentration producing half-maximal effect (EC_{50}) were estimated by fitting the data to Hill equations, using least-square routines as previously described (Palma et al., 2002). I_{ACh} desensitization was measured by fitting ACh currents with Equation 1.

Data were analyzed using Sigma Plot software and are given as means ± SEM.; data sets are considered statistically different when $P< 0.05$. (ANOVA test).

RESULTS

Riluzole effect on whole-cell ACh-evoked currents in HEK cells.

We first examined the influence of riluzole on the function of recombinant human γ- or ε-AChR expressed in HEK cells. ACh (100 μM, 0.5 s) elicited whole cell current (I_{ACh}) responses in virtually all EGFP-positive cells. No consistent difference in current amplitude was observed between cells expressing γ- or ε-AChR, in spite of large cell-to cell variations (range: from -45 to - 0.5 nA at -60 mV for both AChR types). These currents had an exponential decay during sustained ACh applications (Fig. 1A) with time constants of 117 ± 10 ms (γ-AChR, n = 32) and 113 ± 6 ms (ε-AChR, n = 23). At a concentration present in patients' serum (0.5 μM), riluzole coapplied with ACh had almost no effect on I_{ACh}. However, when cells expressing γ-AChR were pretreated with riluzole before it was co-applied with ACh, current amplitude was decreased and its decay accelerated (Fig. 1A; see Supplementary Table 1 for details), so that current integral (Q_{ACh}), which depends on both parameters, was reduced. Even the briefest pretreatment tested (0.5 s) enhanced riluzole effect, which reached a plateau with 5 s preapplications, when Q_{ACh} was reduced to about 50% of control value (Fig. 1B). In cells expressing ε-AChR, riluzole was less effective, as Q_{ACh} was reduced at most to about 70% of control value (Fig. 1B and Supplementary Table 1). For both γ- and ε-AChR, I_{ACh} reduction was enhanced when riluzole concentration was increased to 50 μM (data not shown).

The increase of riluzole-induced effect on I_{ACh} after pretreatment might be due to its interference with intracellular signalling pathways that in turn modulate I_{ACh}. We therefore assessed the effect of riluzole in cells internally dialyzed with GDPβS, a non-phosphorylable analogue of GDP, which prevents G-protein activation. However, inclusion of GDPβS (100 μM) into the patch pipette did not interfere with the effect of riluzole (0.5 μM, 30 s pretreatment, Fig. 1B and C) in transfected cells expressing γ- or ε-AChR, arguing against a G protein-mediated action of riluzole on AChR.

Block of ACh-evoked currents in oocytes

Riluzole-induced reduction of I_{ACh} in cells expressing γ-AChR was similar to that observed in human myotubes (Palma et al., 2011), suggesting that the expression system used does not influence riluzole action. This point was further tested in

Xenopus oocytes expressing γ- or ε-AChR (Fig. 2). Application of ACh to these cells (1 μM to 1 mM for 4 s) elicited inward currents (I_{ACh}) with peak amplitude depending on transmitter concentration, whereas non-injected oocytes showed no detectable responses to ACh. In oocytes expressing ε-AChR, ACh at 50 μM elicited a current with mean peak amplitude of -2.8 ± 0.9 μA (-60 mV; 24 oocytes/ 4 frogs; 24/4). Currents of similar amplitude (-1.7 ± 0.4 μA; 22/4) were recorded from oocytes expressing γ-AChR. As in HEK cells, riluzole affected I_{ACh} and the block was enhanced if the drug was applied before ACh. In oocytes, the plateau was attained at 120 s of pretreatment, which was used in all experiments described below. Riluzole-induced inhibition of I_{ACh} was more potent in oocytes expressing γ-AChRs than ε-AChRs, as shown by concentration-response curves (Fig. 2) that yielded IC_{50} values of 8.0 ± 1.1 μM (n = 8/3) and 55.6 ± 0.7 μM (n = 10/3), respectively (P = 0.00001); n_H was about 1.5 for both AChR isoforms. For both AChR types, the effect of riluzole was voltage-independent in the range -100 to + 20 mV (8 oocytes each; data not shown).

In oocytes expressing ε-AChR the decay of I_{ACh} was not modified by riluzole at its IC_{50} (50 μM), as τ_{decay} was 1.7 ± 0.3 s and 1.5 ± 0.4 s (n = 8/3; P=0.3) before and in the presence of riluzole, respectively. By contrast, in oocytes expressing γ-AChR the riluzole-induced decrease of I_{ACh} was accompanied by a significant change in current decay, as τ_{decay} was 1.8 ± 0.2 s (n = 8/3) under control conditions and, in the same oocytes, it became 0.7 ± 0.1 s (P=0.002) during treatment with riluzole (10 μM), resembling the effect described in transfected HEK cells.

The block of I_{ACh} was independent of ACh concentration (1 μM to 1 mM) to and riluzole (50 μM) did not affect the potency of ACh on γ- or ε-AChR, since ACh concentration - current response relationships yielded similar values of EC_{50} and n_H (16.7 ± 1.1 μM and 1.1 ± 0.1, n=6/2 for ε-AChR; 21.5 ± 0.2 μM and 1.6 ± 0.2, n=6/2 for γ-AChR) before and during riluzole treatment (data not shown). These observations suggest that the riluzole-induced acceleration of current decay is not related to a change in neurotransmitter potency.

Effect on unitary ACh-evoked events in HEK cells and human myotubes

The mechanism of riluzole action on I_{ACh} was investigated analysing unitary ACh-evoked events either in the cell attached or outside-out configuration. Outside-out

recordings were performed on HEK cells expressing γ- or ε-AChR, subsequently exposed to ACh (100 nM at -80 mV) or ACh plus riluzole (0.5 μM), with at least 10 s wash between applications. In each patch, unitary events evoked by ACh alone or plus riluzole had identical conductance (39.6 ± 0.7 pS, n=11 for γ-AChR; 50.0 ± 1.0, n=7 for ε-AChR) and open time distribution (Table 1). However, in the presence of riluzole, closed time histograms were shifted to the right in all patches, as compared to control conditions (Figure 3), although only the third and fourth (for γ-AChR) best fitting exponential components were significantly prolonged (Table 1). Riluzole-induced increase of channel closed duration was not an artefact due to channel run-down, as in most patches closed times reversed towards control values when ACh was applied alone for a second time (data not shown). It must be noted that in these experiments, riluzole preapplication was not used, but the initial 5-10 s of the recordings, when multiple ACh-induced openings occurred, were not considered for analysis.

To check that riluzole effect is not influenced by patch excision, we performed cell-attached recordings on HEK cells expressing γ-AChR, including riluzole (0.5 μM) in the patch pipette. Again, unitary channel conductance was identical in control and riluzole-exposed patches (34.0 ± 3.1 pS and 32.2 ± 0.9 pS, respectively; n=7 for both). The distribution of open durations was adequately fitted by 2 exponential components with similar time constants in the two experimental groups (Figure 4A; details in Supplementary Table 2). Closed time distribution was widely variable for both control and treated cells, and could not be reliably compared. Cell-attached recordings were performed also on myotubes from ALS patients (Figure 4B) and yielded analogous results. In these cells, most experiments were performed bathing cells in KCl-based extracellular solution. Channel conductance was 35.7 ± 1.1 pS (n=13) under control conditions and 33.0± 3.1 pS (n=7) with riluzole. In both control and riluzole-exposed patches, open time distributions were fitted by 2 exponential components with time constants similar to those observed in HEK cells, and not influenced by the drug (Figure 4B; details in Supplementary Table 2).

How fast is riluzole action?

During neuromuscular transmission, nerve-released ACh is present in the synaptic cleft only for few ms before being hydrolyzed by acetylcholinesterase. The action of

riluzole on such a fast time scale cannot be inferred from whole-cell recordings, as rise-time of ACh-evoked currents is in the order of 10-20 ms. Macroscopic ACh-evoked currents from outside-out patches have a much shorter rise time, and we could assess the effect of riluzole (0.5 μM, 30 s pretreatment) within few ms of ACh (100 μM) application (Figure 5). In membrane patches expressing ε-AChR, in the presence of riluzole Q_{ACh} was 96 ± 3 % (n=8) of control value after 10 ms of ACh application but it was significantly reduced to 83 ± 6 % (n=8, P=0.02) at 100 ms, indicating that the action of the drug develops slowly. For γ-AChR, Q_{ACh} was significantly reduced to 79 ± 4 % of control value (n=6, P=0.002) at 10 ms and to 66 ± 3 % (n=6, P=0.0001) at 100 ms.

Riluzole does not affect CMAPs in ALS patients

To examine if riluzole as used in clinical practice affects neuromuscular transmission, we examined 36 ALS patients, measuring the amplitude of compound muscle action potentials (CMAPs) elicited by repetitive nerve stimulation (RNS), which provides a sensitive and non-invasive assay of neuromuscular transmission. Patients were tested immediately before and after 1-week suspension of riluzole treatment, a time that allows for adequate riluzole washout, which has been estimated at about 40 hours (Le Liboux et al., 1999; Chandu et al., 2010). The test was performed on two different nerve-muscle groups. After the week of riluzole washout, CMAP amplitude did not change significantly in any of the patients examined, showing that no further axonal depletion occurred between the two neurophysiological evaluations. The decrease of CMAP amplitude during RNS was also not statistically different at the end of the riluzole washout period as compared to the control value, for both the ulnar and the axillary nerves (Figure 6). Thus, riluzole treatment appears to be devoid of detrimental effects at least on this estimator of neuromuscular transmission.

DISCUSSION

The results of this paper disclose a differential effect of riluzole on recombinant human γ-AChR and ε-AChR, expressed in HEK cells or oocytes. In both cell systems, riluzole-induced block was faster and stronger for γ-AChR than for ε-AChR, although with kinetic differences between the two cell types, likely due to the large size and complex membrane of oocytes as compared to HEK cells. In outside-out recordings, the synaptic AChR isoform was blocked by riluzole only with ACh applications far outlasting the typical duration of synaptic events, allowing the hypothesis that riluzole at clinical concentrations should not impair endplate function. This supposition was verified in vivo, measuring CMAPs elicited by nerve stimulation in ALS patients, to determine the efficiency of neuromuscular transmission. In agreement with our hypothesis, muscle response to nerve stimulation was not influenced by 1-week suspension of riluzole treatment, which produces complete washout of plasma riluzole (Le Liboux et al., 1999; Chandu et al., 2010). Furthermore, the absence of effects on CMAPs evoked by repetitive nerve stimulation suggests that clinical use of riluzole does not affect the safety factor at the neuromuscular junction in treated patients.

As previously seen in human tissue (Palma et al., 2011), we show here that preapplication of riluzole increases the block of I_{ACh} in cells expressing recombinant γ- or ε-AChR. This observation raises the possibility that intracellular signalling pathways mediate riluzole-induced block of AChR. For instance, in neuronal membranes riluzole blocks PKC (Noh et al., 2000). However, in transfected HEK cells, riluzole effect was preserved upon patch excision or blockade of G-proteins by the classical inhibitor GDPβS, indicating that soluble intracellular factors and G-proteins are not involved in the transduction of riluzole effect. Moreover, the effect on I_{ACh} was observed in experimental systems as diverse as cDNA-injected oocytes (this work) and cultured human myotubes (Palma et al., 2011), which seems to be more consistent with a direct action of riluzole on AChR than with the transduction by a second messenger.

Being independent of ACh concentration, at least in oocytes, riluzole-induced block of I_{ACh} appears to be due to a non-competitive mechanism of action. Open-channel block is an unlikely candidate, as riluzole has a voltage-independent effect and does not influence the duration of ACh-evoked channel openings, the two hallmarks of open-channel blockade (Neher and Steinbach, 1978). In oocytes, riluzole did not

change ACh potency at γ- or ε-AChR, suggesting that ACh binding and channel gating are largely unaltered for both receptors (Colquhoun, 1998); therefore AChR desensitization was likely the functional parameter affected by riluzole. Single-channel recordings showed that riluzole had no effect on the conductance and open time distribution of ACh-evoked channels, but prolonged closed intervals, supporting the hypothesis that it acts by stabilizing AChR desensitized state(s), with no effect on the open state. Such an action has already been proposed for other substances, which have an enhanced effect on AChR channels following preapplication, for instance 3-(trifluoromethyl)-3-(m-iodophenyl)diazirine, some local anesthetics and verapamil (Forman, 1999; Spitzmaul et al., 2009; Moriconi et al., 2010;)

Both in oocytes and in HEK cells, riluzole blocked the γ-AChR more than the ε-AChR, thus adding to the list of compounds having differential actions on the two isoforms of muscle AChR. For instance, the γ-AChR is more sensitive than the ε-AChR to block by 5-hydroxytryptamine (Grassi, 1999) or hydrocortisone (Bouzat and Barrantes, 1996); fluoxetine alters channel kinetics of the γ-AChR (Garcia-Colunga et al., 1997) but not the ε-AChR (Harper et al., 2003). More striking, d-tubocurarine at low concentrations is a blocker of ε-AChR, but a weak agonist of γ-AChR (Steinbach and Chen, 1995).

While we show that riluzole-induced block of ε-AChR is unlikely to occur during neuromuscular transmission, blockade of γ-AChR may play some role in disease history. Since muscle fibres of ALS patients undergo denervation and subsequent reinnervation by collateral sprouting of healthy motor neurones (Eisen and Swash, 2001), the γ-AChR isoform may transiently coexist with ε-AChR at reinnervated endplates, as it happens in rodents (Yampolsky et al., 2010). However, also for γ-AChR, brief ACh-evoked currents were little affected by clinical concentrations of riluzole, again suggesting that synaptic transmission is unlikely to be impaired. In non-innervated muscles, activation of extrasynaptic γ-AChR might be induced by the tonic release of ACh or an ACh-like compound, well documented in cultured myotubes and denervated muscle *in vivo* (Krnjevic and Straughan, 1964; Krause et al., 1995; Bandi et al., 2005). Whether or not γ-AChRs influence muscle reinnervation in humans is unknown; in rodents reinnervation of partially denervated muscles is impaired by α-bungarotoxin (Connold and Vrbova, 1991). Other studies, however, point out that full chronic AChR blockade is required to prevent collateral sprouting

of motor axons (Pestronk and Drachmann, 1985), so that the partial riluzole-induced reduction of AChR function might be non detrimental to the reinnervation process, an hypothesis that deserves analysis in adequate experimental systems. On the other hand, it has long been known that, during chick and mouse development, blockade or reduction of γ-AChR favours motor neuron survival (Oppenheim et al., 2000; Terrado et al., 2001; Liu et al., 2008; Yampolsky et al., 2008), thus allowing the suggestion that riluzole action might be beneficial against ongoing motor neuron degeneration through this route, too.

At present, the idea that muscle denervation may precede -or even contribute to- motor neuron death is gaining support (as reviewed by Musarò, 2010; Dadon-Nachum et al., 2011), so that investigation of the physiological consequences of riluzole-induce blockade of γ-AChR warrants further studies to understand whether it contributes, positively or negatively, to disease progression.

REFERENCES

1) Bandi E, Bernareggi A, Grandolfo M, Mozzetta C, Augusti-Tocco G, Ruzzier F, Lorenzon P (2005) Autocrine activation of nicotinic acetylcholine receptors contributes to Ca^{2+} spikes in mouse myotubes during myogenesis. *J Physiol* **568**, 171-180.
2) Bellingham MC (2011) A review of the neural mechanisms of action and clinical efficiency of riluzole in treating amyotrophic lateral sclerosis: what have we learned in the last decade? *CNS Neurosci Ther* **17**, 4-31.
3) Bouzat C, Barrantes FJ (1996) Modulation of muscle nicotinic acetylcholine receptors by the glucocorticoid hydrocortisone. Possible allosteric mechanism of channel blockade. *J Biol Chem* **271**, 25835-25841.
4) Chandu BR, Nama S, Kanala K, Challa BR, Shaik RP, Khagga M (2010) Quantitative estimation of riluzole in human plasma by LC-ESI-MS/MS and its application to a bioequivalence study. *Anal Bioanal Chem* **398**, 1367-1374.
5) Connold AL, Vrbova G (1991) Temporary loss of activity prevents the increase of motor unit size in partially denervated rat soleus muscles. *J Physiol* **434**, 107-119.
6) Colquhoun D (1998) Binding, gating, affinity and efficacy: The interpretation of structure-activity relationships for agonists and of the effects of mutating receptors. *Br J Pharmacol* **125**, 924-947.
7) Dadon-Nachum M, Melamed E, Offen D (2011) The "dying-back" phenomenon of motor neurons in ALS. *J Mol Neurosci* **43**, 470-477.
8) Di Angelantonio S, Piccioni A, Moriconi C, Trettel F, Cristalli G, Grassi F, Limatola C (2011) Adenosine A2A receptor induces protein kinase A-dependent functional modulation of human (alpha)3(beta)4 nicotinic receptor. *J Physiol* **589**, 2755-2766.
9) Di Castro A, Martinello K, Grassi F, Eusebi F, Engel AG (2007) Pathogenic point mutations in a transmembrane domain of the epsilon subunit increase the Ca^{2+} permeability of the human endplate ACh receptor. *J Physiol* **579**, 671-677.
10) Eisen A, Swash M (2001) Clinical neurophysiology of ALS. *Clin Neurophysiol*, **112**, 2190-2201.
11) Forman SA (1999) A hydrophobic photolabel inhibits nicotinic acetylcholine receptors via open-channel block following a slow step. *Biochemistry* **38**, 14559-14564.

12) Fucile S, Sucapane A, Grassi F, Eusebi F, Engel AG (2006) The human adult subtype ACh receptor channel has high Ca^{2+} permeability and predisposes to endplate Ca^{2+} overloading. *J Physiol* **573**, 35-43.

13) García-Colunga J, Awad JN, Miledi R (1997) Blockage of muscle and neuronal nicotinic acetylcholine receptors by fluoxetine (Prozac). *Proc Natl Acad Sci USA*, **94:** 2041-2044

14) Grassi F (1999) 5-hydroxytryptamine blocks the fetal more potently than the adult mouse muscle acetylcholine receptor. *Pflugers Arch* **437**, 903-909.

15) Harper CM, Fukodome T, Engel AG (2003) Treatment of slow-channel congenital myasthenic syndrome with fluoxetine. *Neurology* **60**, 1710-1713.

16) Katz B, Miledi R (1964) Further observations on the distribution of actylcholine-reactive sites in skeletal muscle. *J Physiol* **170**, 379-388

17) Krause RM et al. (1995) Activation of nicotinic acetylcholine receptors increases the rate of fusion of cultured human myoblasts. *J Physiol* **489**, 779-790.

18) Krnjevic K and Straughan DW (1964) The release of acetylcholine from the denervated rat diaphragm. *J Physiol* **170**, 371-378.

19) Le Liboux A, Cachia JP, Kirkesseli S, Gautier JY, Guimart C, Montay G, Peeters PA, Groen E, Jonkman JH, Wemer J (1999) A comparison of the pharmacokinetics and tolerability of riluzole after repeat dose administration in healthy elderly and young volunteers. *J Clin Pharmacol* **39**, 480-486.

20) Liu Y, Padgett D, Takahashi M, Li H, Sayeed A, Teichert RW, Olivera BM, McArdle JJ, Green WN, Lin W (2008) Essential roles of the acetylcholine receptor gamma-subunit in neuromuscular synaptic patterning. *Development* **135**, 1957-1967.

21) Miledi R, Palma E, Eusebi F (2006) Microtransplantation of neurotransmitter receptors from cells to Xenopus oocyte membranes: new procedure for ion channel studies. *Methods Mol Biol* **322**, 347-355.

22) Mohammadi B, Lang N, Dengler R, Bufler J (2002) Interaction of high concentrations of riluzole with recombinant skeletal muscle sodium channels and adult-type nicotinic receptor channels. *Muscle Nerve* **26**, 539-545.

23) Moriconi C, Di Castro MA, Fucile S, Eusebi F, Grassi F (2010) Mechanism of verapamil action on wild-type and slow-channel mutant human muscle acetylcholine receptor. *J Neurochem* **114**, 1231-1240.

24) Musarò A (2010) State of the art and the dark side of amyotrophic lateral sclerosis. *World J Biol Chem* **1**, 62-68.

25) Neher E, Steinbach JH (1978) Local anaesthetics transiently block currents through single acetylcholine-receptor channels. *J Physiol* **277**, 153-176.

26) Noh KM, Hwang JY, Shin HC, Koh JY (2000) A novel neuroprotective mechanism of riluzole: direct inhibition of protein kinase C. *Neurobiol Dis* **7**, 375-383.

27) Oppenheim RW, Prevette D, D'Costa A, Wang S, Houenou LJ, McIntosh JM (2000) Reduction of neuromuscular activity is required for the rescue of motoneurons from naturally occurring cell death by nicotinic-blocking agents. *J Neurosci* **20**, 6117-6124.

28) Palma E et al. (2002) Expression of human epileptic temporal lobe neurotransmitter receptors in Xenopus oocytes: An innovative approach to study epilepsy. *Proc Natl Acad Sci USA* **99**, 15078-15083.

29) Palma E, Inghilleri M, Conti L, Deflorio A, Frasca V, Manteca A, Pichiorri F, Roseti C, Torchia G, Limatola C, Grassi F, Miledi R (2011) Physiological characterization of human muscle acetylcholine receptors from ALS patients. *Proc Natl Acad Sci USA*, DOI: 10.1073/pnas.1117975108.

30) Pestronk A, Drachman DB (1985) Motor nerve terminal outgrowth and acetylcholine receptors: inhibition of terminal outgrowth by alpha-bungarotoxin and anti-acetylcholine receptor antibody. *J Neurosci* **5**, 751-758.

31) Spitzmaul G, Gumilar F, Dilger JP, Bouzat C (2009) The local anaesthetics proadifen and adiphenine inhibit nicotinic receptors by different molecular mechanisms. *Br J Pharmacol* **157**, 804-817

32) Steinbach JH, Chen Q (1995) Antagonist and partial agonist actions of d-tubocurarine at mammalian muscle acetylcholine receptors. *J Neurosci* **15**, 230-240.

33) Terrado J, Burgess RW, DeChiara T, Yancopoulos G, Sanes JR, Kato AC (2001) Motoneuron survival is enhanced in the absence of neuromuscular junction formation in embryos. *J Neurosci* **21**, 3144-3150.

34) Witzemann V, Brenner HR, Sakmann B (1991) Neural factors regulate AChR subunit mRNAs at rat neuromuscular synapses. *J Cell Biol* **114**, 125-141.

35) Yampolsky P, Gensler S, McArdle J, Witzemann V (2008) AChR channel conversion and AChR-adjusted neuronal survival during embryonic development. *Mol Cell Neurosci* **37**, 634-645.

36) Yampolsky P, Pacifici PG, Witzemann V (2010) Differential muscle-driven synaptic remodeling in the neuromuscular junction after denervation. *Eur J Neurosci* **31**, 646-658.

AUTHOR CONTRIBUTIONS

FG, EP, MI and CL planned and discussed experiments; CD, LC, CR and AM performed experiments and critically analyzed the data; EG and MI examined patients; MI performed biopsies; FG, EP and MI wrote the paper; all authors approved the manuscript.

AKNOWLEDGMENTS

The Authors thank all the patients who made this study possible by donating muscle tissue. This work was supported by grants from Association Française contre le Myopathies (FG), Fondazione Viva la Vita (to MI and CL), Ministero della Salute Antidoping project (to CL and EP), Ministero dell'Istruzione, dell'Università e della Ricerca (MIUR-PRIN grants to EP and CL). CD and LC were supported by the PhD Program in Neurophysiology at Sapienza University, Rome. The Authors declare no conflict of interests.

Table 1: Riluzole action on AChR-channel kinetics in outside-out patches.

	ε-AChR (7 patches)		γ-AChR (11 patches)	
	Control	Riluzole	Control	Riluzole
τ_{open1} (ms) (a_{open1}) (%)	0.50 ±0.05 (55 ± 5)	0.50± 0.02 (45 ± 5)	0.7 ±0.1 (40 ± 2)	0.7 ± 0.1 (40 ± 2)
τ_{open2} (ms) (a_{open2}) (%)	1.8 ± 0.2 (45 ± 5)	1.7 ± 0.1 (55±5)	3.5 ± 0.4 (60 ± 2)	3.9 ± 0.5 (60 ± 2)
$\tau_{closed1}$ (ms) ($a_{closed1}$) (%)	0.20 ± 0.02 (16 ± 1	0.30 ± 0.06 (20 ± 3)	0.20 ± 0.08 (21 ± 3)	0.5 ± 0.2 (8 ± 1)
$\tau_{closed2}$ (ms) ($a_{closed2}$) (%)	1.8 ± 0.3 (34 ± 3)	2.8 ± 0.5 (31 ± 5)	3.9 ± 0.9 (22 ± 4)	6.2 ± 1.1 (21 ± 4)
$\tau_{closed3}$ (ms) ($a_{closed3}$) (%)	8.7 ± 1.9 (48 ± 2)	18 ± 5 * (47 ± 4)	33 ± 6 (39 ± 3)	61 ± 12 * (43 ± 3)
$\tau_{closed4}$ (ms) ($a_{closed4}$) (%)			219 ± 50 (23 ± 4)	420 ± 100* (31 ± 7)

τ_{open} (a_{open}) and τ_{closed} (a_{closed}): time constants (weight) of the exponential components best fitting the distribution of open and closed durations, respectively. Data are given as mean ± S.E.M. for the indicated number of patches, each exposed to ACh (100 nM, -80 mV) alone and to ACh plus riluzole (0.5 μM). *: Significantly larger than control ($P<0.04$, paired Student's *t* test)

FIGURES AND LEGENDS

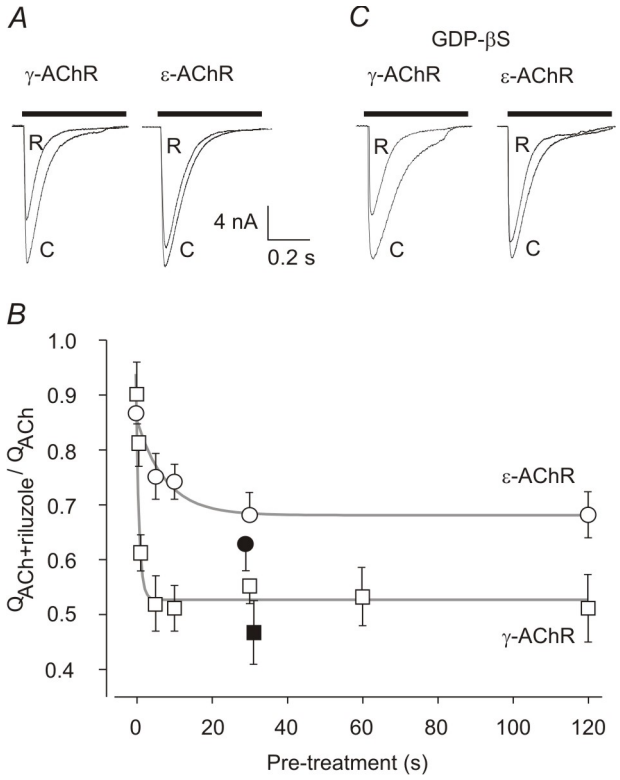

Figure 1. Effect of riluzole on ACh-evoked whole-cell currents in HEK cells.

A, typical whole-cell currents evoked by ACh (100 μM, horizontal bar) alone (C) or in the presence of riluzole (R; 0.5 μM, 30 s pre-treatment) in cells expressing the indicated AChR type. *B*, duration of pre-treatment with riluzole (0.5 μM) enhances its effect in cells expressing γ- or ε-AChR as indicated (filled symbols: inclusion of GDPβS into the patch pipette). The integral of current response (Q_{ACh} or $Q_{ACh+riluzole}$) was calculated over the entire duration of ACh (100 μM) application; riluzole effect was quantified by the ratio $Q_{ACh+riluzole}/Q_{ACh}$ in each cell (4 to 10 for each point). Grey line represents the exponential best fit of the experimental points. *C,* typical whole-cell currents evoked by ACh alone or plus riluzole (as in *A*) when GDPβS (100 μM) was included the patch pipette. Notice that riluzole effect is preserved. In all panels, holding potential, -60 mV.

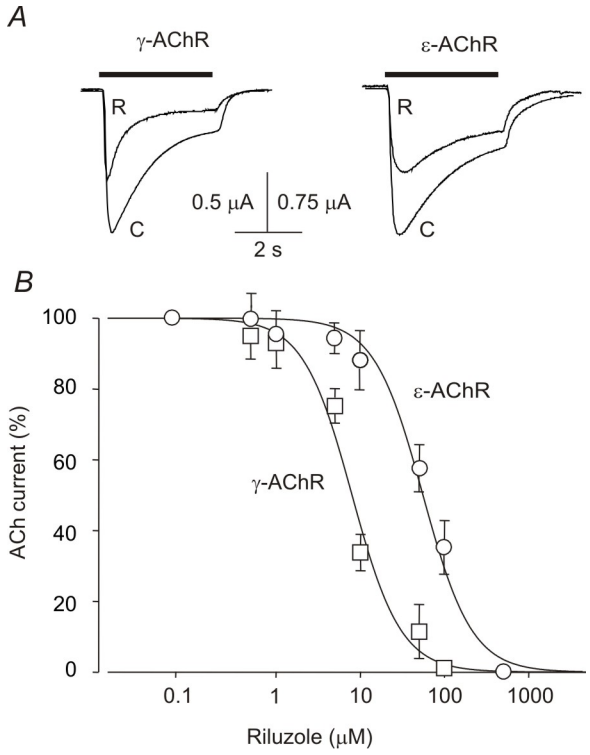

Figure 2. Inhibition of ACh-evoked currents by riluzole in oocytes.

A, typical currents evoked by ACh (horizontal bars) alone (C) or together with riluzole (R; 50 μM for ε-AChR; 10 μM for γ-AChR; 120 s pretreatment for both) in two oocytes expressing AChRs as indicated. *B*, plot of relative amplitude of currents evoked by ACh (50 μM, -60 mV) plus riluzole at various concentrations (120 s pretreatment), expressed as percent of control current (ACh alone) in the same cell, for oocytes expressing γ-AChR (□, 8/3) or ε-AChR (○, 10/3). IC_{50} and n_H were 8.0 ± 1.1 μM and 1.5 ± 0.2 (γ-AChR); 55.6 ± 0.7 μM and 1.5 ± 0.3 (ε-AChR).

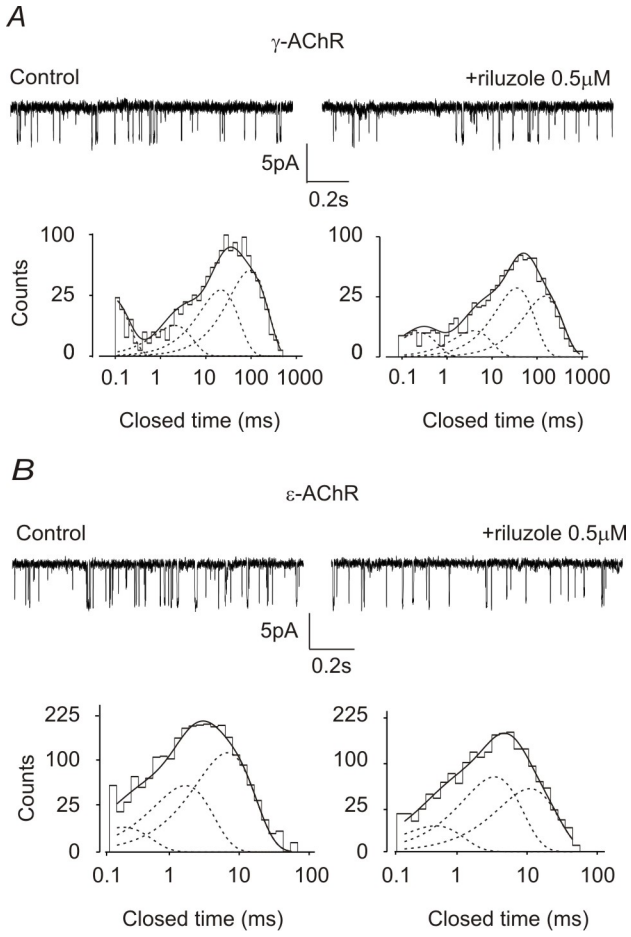

Figure 3. Effect of riluzole on unitary ACh-evoked currents in outside-out patches. *A* and *B*, unitary events evoked by ACh (100 nM, -80 mV) in outside-out patches expressing γ-AChR (*A*) or ε-AChR (*B*), sequentially exposed to ACh alone (control) or plus riluzole (0.5 μM), as indicated. Bottom panels represent the histograms of channel closed times, obtained in the recordings shown above, best fitted with four (γ-AChR) or three (ε-AChR) exponential components. Notice the lengthening of the closed times in the presence of riluzole, as compared to control conditions. Channel openings represented by downward deflections.

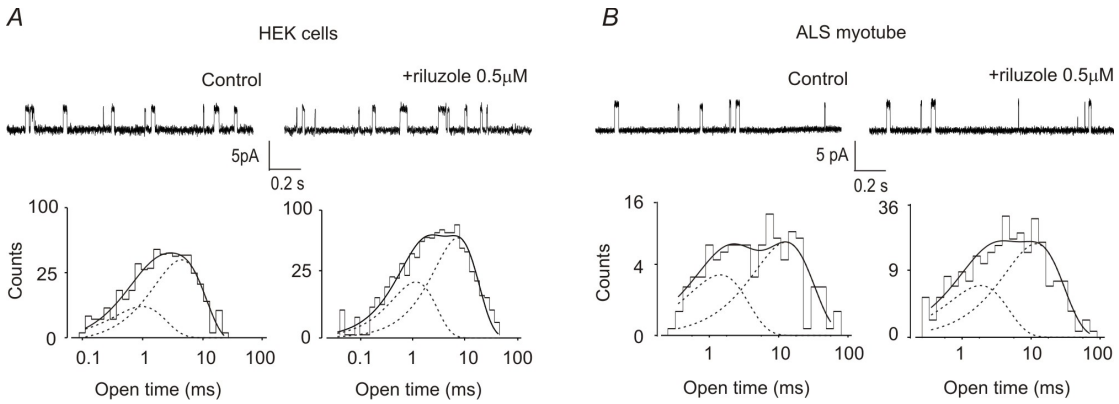

Figure 4. Effect of riluzole in cell-attached recordings.

A, typical cell-attached recordings in two different HEK cells expressing γ-AChR, including in the patch pipette ACh (100 nM) alone (slope conductance, 31 pS) or plus riluzole (0.5 μM; slope conductance, 34 pS), as indicated. *Bottom*, the histograms of channel open durations, obtained in the same recordings, were best fitted by two exponential components, with time constants τ_{op1} = 1.5 ms (33%) and τ_{op2} = 9.5 ms (67%) for control; 1.1 ms (35%) and 7.4 ms (65%) in presence of riluzole. *B*, cell-attached recording of unitary events in two different patches on the same myotube from an ALS patient, using ACh (100 nM) alone or plus riluzole, as indicated. Channel conductance was 30 pS (control) or 34 pS (+ riluzole). *Bottom*, the corresponding histograms of channel opening durations, best fitted by two exponential components with τ_{op1} = 1.4 ms (39%) and τ_{op2} = 12.7 ms (61%) in control conditions, 1.8 ms (36%) and 11.7 ms (64%) in the presence of riluzole. In all panels, channel openings are represented by upward deflections; cells were bathed in standard external solution.

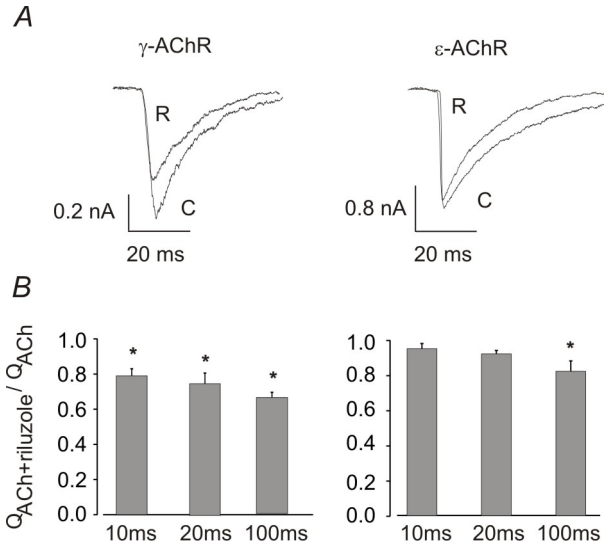

Figure 5. Effect of riluzole during fast ACh applications.

A, superimposed currents evoked by sequential applications of ACh (100 μM, 100 ms) alone (C) or together with riluzole (R; 0.5 μM, 30 s pre-treatment) to outside-out patches from HEK cells expressing γ- or ε-AChR, as indicated. *B*, bar graphs representing relative current integral during 10, 20 and 100 ms from ACh application. For γ-AChR, riluzole-induced reduction of Q_{ACh} was significant already at 10 ms (*: $P < 0.002$); for ε-AChR, current integral was significantly reduced only at 100 ms (*: $P=0.02$). In all panels, holding potential, -60 mV.

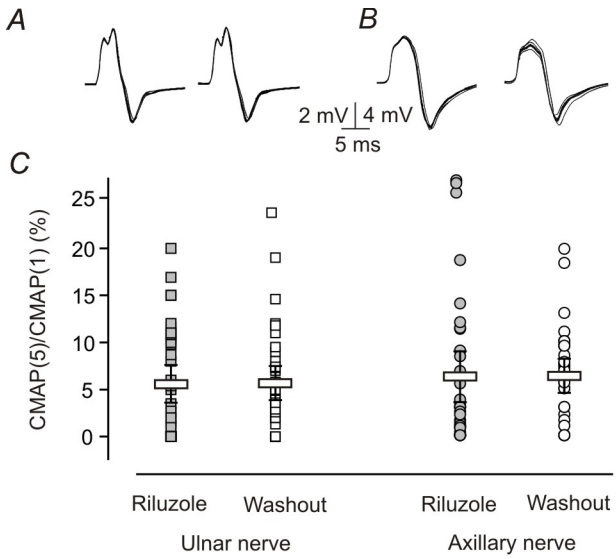

Figure 6. Riluzole has no effect on neuromuscular transmission in ALS patients. *A* and *B*, Superimposed traces representing 10 CMAPs evoked by repetitive stimulation of the ulnar (*A*) and axillary nerve (*B*) in a patient, during riluzole treatment (left) and at the end of a 1-week medicament washout. Notice that CMAP amplitude remains constant in this individual. *C*, dispersion plot of CMAP evoked by the 5th stimulus, expressed as percent of the amplitude of the 1st response, for all 36 patients considered in the study. Boxes represent mean ± 95% confidence interval of all values. For both ulnar and axillary nerves, values were not modified by riluzole washout (P> 0.9).

Supplementary Table 1: Pre-application of riluzole increases its effect on I_{ACh} amplitude and decay.

	ε-AChR		γ-AChR	
Pretreatment (s)	Amplitude (%)	τ_{decay} (%)	Amplitude (%)	τ_{decay} (%)
0	100 ± 3 (n=7)	83 ± 4	92±5 (n=7)	97±2
0.5	87, 81	70, 79	78±3 (n=10)*	100±5
1	NA	NA	67±2 (n=10)$^{\#}$	81±2$^{\#}$
5	88±6 (n=4)	89±3*	54±5 (n=9)$^{\#}$	74±3$^{\#}$
10	93±7 (n=5)	80±3$^{\#}$	55±5 (n=8)*	75±3*
30 +GDPβS	86±3 (n=5)* 84±5 (n=5)*	71±4$^{\#}$ 69 ± 4*	72±4 (n=14)$^{\#}$ 70±10* (n=4)	75±3$^{\#}$ 63±2$^{\#}$
60	NA	NA	69±5 (n=12)$^{\#}$	73±2$^{\#}$
120	97 ± 3 (n=6)	79 ± 8 *	69±6 (n=8)$^{\#}$	73±3$^{\#}$

Data are mean ± SEM values (number of cells tested) of the amplitude and decay time constant (t_{decay}) of whole-cell currents elicited by ACh (100 μM at -60 mV) in HEK cells expressing the indicated AChR type. Values obtained in the continuous presence of riluzole (0.5 μM), preapplied for the indicated amount of time, are expressed as percent of the values obtained under control conditions (ACh alone) in each cell. Comparison of data obtained with riluzole *vs.* control values was tested using paired Student's *t* test; *: $P<0.05$; #: $P < 0.005$,

Supplementary Table 2: Open channel distribution in cell-attached recordings

	HEK cells		ALS myotubes	
	τ_1 (ms) (a_1) (%)	τ_2 (ms) (a_2) (%)	τ_1 (ms) (a_1) (%)	τ_2 (ms) (a_2) (%)
Control	1.4 ± 0.1 (n=6) (33 ± 4)	7.0 ± 0.7 (67 ± 4)	1.2 ± 0.1 (n=5) (34 ± 2)	9.4 ± 0.5 (66 ± 3)
riluzole	1.4 ± 0.2 (n=7) (43 ± 4)	7.6 ± 0.8 (57 ± 4)	2.0 ± 0.5 (n=7) (38 ± 5)	12.2 ± 0.9 (62 ± 5)

τ_1 (a_1) and τ_2 (a_2): time constants (weight) of the two exponential components best fitting the distribution of channel open durations, in HEK cells transfected with γ-AChR or in myotubes derived from satellite cells of ALS patients. Data are given as mean ± S.E.M. for the indicated number of patches, each exposed to ACh (100 nM, -80 mV) alone or to ACh plus riluzole (0.5 μM). In both cell types, values obtained with riluzole were not significantly different ($P > 0.06$) from the corresponding values in control recordings.